TISSUE ENGINEERING: Part A
Volume 19, Numbers 1 and 2, 2013

DOI: 10.1089/ten.tea.2011.0412

Human Embryonic Stem Cell-Derived Mesodermal Progenitors Display Substantially Increased Tissue Formation Compared to Human Mesenchymal Stem Cells Under Dynamic Culture Conditions in a Packed Bed/Column Bioreactor

Giuseppe Maria de Peppo, Ph.D.,[1–3,*] Martina Sladkova, M.Sc.,[4,*] Peter Sjövall, Ph.D.,[3,5] Anders Palmquist, Ph.D.,[2,3] Karim Oudina, Ph.D.,[4] Johan Hyllner, Ph.D.,[6] Peter Thomsen, Ph.D.,[2,3] Hervé Petite, Ph.D.,[4] and Camilla Karlsson, Ph.D.[2,3]

Bone tissue engineering represents a promising strategy to obviate bone deficiencies, allowing the *ex vivo* construction of bone substitutes with unprecedented potential in the clinical practice. Considering that in the human body cells are constantly stimulated by chemical and mechanical stimuli, the use of bioreactor is emerging as an essential factor for providing the proper environment for the reproducible and large-scale production of the engineered substitutes. Human mesenchymal stem cells (hMSCs) are experimentally relevant cells but, regardless the encouraging results reported after culture under dynamic conditions in bioreactors, show important limitations for tissue engineering applications, especially considering their limited proliferative potential, loss of functionality following protracted expansion, and decline in cellular fitness associated with aging. On the other hand, we previously demonstrated that human embryonic stem cell-derived mesodermal progenitors (hES-MPs) hold great potential to provide a homogenous and unlimited source of cells for bone engineering applications. Based on prior scientific evidence using different types of stem cells, in the present study we hypothesized that dynamic culture of hES-MPs in a packed bed/column bioreactor had the potential to affect proliferation, expression of genes involved in osteogenic differentiation, and matrix mineralization, therefore resulting in increased bone-like tissue formation. The reported findings suggest that hES-MPs constitute a suitable alternative cell source to hMSCs and hold great potential for the construction of bone substitutes for tissue engineering applications in clinical settings.

Introduction

Engineering bone tissue requires interfacing stem cells to biomaterials as suitable scaffolds for the cells to attach, proliferate, and differentiate toward the osteogenic lineage. To prime stem cells toward the signaling pathway leading to osteogenic differentiation, the cell/scaffold constructs are eventually treated with appropriate chemicals *in vitro*.[1] Nonetheless, the development of dynamic culture strategies is emerging as an essential factor to improve proliferation and differentiation of the cells in the scaffold by enabling nutrient supply, providing mechanical stimulation and a proper environment for the reproducible and large-scale production of the engineered tissues. In fact, cells in the human body are constantly subjected to chemical and mechanical stimuli, which ensure cell functionality and contribute to tissue organization.[2,3] Therefore, the use of bioreactors is becoming a fundamental step for the fabrication of three-dimensional (3D) cell/scaffold constructs for tissue engineering applications. Different bioreactor

[1]The New York Stem Cell Foundation, New York, New York.
[2]Department of Biomaterials, Sahlgrenska Academy at University of Gothenburg, Gothenburg, Sweden.
[3]BIOMATCELL VINN Excellence Center of Biomaterials and Cell Therapy, Göteborg, Sweden.
[4]Laboratoire de Bioingéniérie et Biomécanique Ostéoarticulaires, CNRS UMR 7052 Faculté de médecine, Paris Denis Diderot, Paris, France.
[5]Chemistry and Materials Technology, SP Technical Research Institute of Sweden, Borås, Sweden.
[6]Cellartis AB, Gothenburg, Sweden.
*These two authors contributed equally to the study and both should be considered first author.

systems have been designed and used for the cultivation of bone-engineered substitutes, including spinner flasks, and rotating vessels, perfusion and compression systems, each providing specific mechanical stresses and regimes for the proper stimulation of the cell/scaffold constructs (for a review see Ref.[4]).

The ability of human mesenchymal stem cells (hMSCs), residing in bone marrow and other adult tissues,[5–8] to differentiate toward the osteogenic lineage[9] makes them suitable for bone engineering applications. Several groups have recently demonstrated the positive effect of perfusion bioreactors on hMSCs concerning enhanced proliferation and osteogenic differentiation.[10–13] However, despite the many encouraging results reported, hMSCs manifest important limitations from a tissue engineering perspective. After aspiration from patients or donors, hMSCs must be isolated and enriched through not yet fully established procedures, usually resulting in a high degree of heterogeneity, which may interfere with an optimal clinical outcome.[14,15] Moreover, limited proliferation potential,[16] progressive loss of functionality upon *in vitro* expansion,[17–19] and age-associated decline in cellular fitness[20] restrict their use for the large-scale construction of bone substitutes. Other than hMSCs, human embryonic stem cells (hESCs) hold the promise to provide a homogenous and unlimited source of cells for bone engineering applications.[21,22] However, their ability to form teratoma *in vivo*[23] is today hampering their potential use in clinical applications. An alternative could be the use of progenitor cells derived from hESCs. To date, many efforts have been made to derive such progenitors using different strategies, such as transfection with human telomerase reverse transcriptase,[24] coculture with mouse OP9 cells,[25] exposure of hESCs to specific supplements,[26,27] fluorescence activated cell sorting,[28] and manual selections of specific cell populations from hESCs colonies or embryoid bodies.[29] We similarly derived mesodermal progenitor cells denoted human embryonic stem cell-derived mesodermal progenitor (hES-MPs) that, unlike other hESC-derived mesodermal progenitors, can be derived through a simple, robust and reproducible protocol under xeno-free conditions,[30] which is a fundamental prerequisite for application of stem cells in clinical situations. hES-MPs do not form teratoma *in vivo* but highly resemble hMSCs in terms of gene expression, surface marker profile,[31] and ability to differentiate toward mesodermal tissues.[30] However, hES-MPs display significantly higher proliferation ability and faster mineralization capacity *in vitro*, in addition to displaying lower amount of HLA class II proteins compared to hMSCs,[31,32] suggesting that hES-MPs may be well qualified for the successful treatment of musculoskeletal conditions.

Beside this, no data exist today regarding the behavior of hES-MPs when cultured on 3D scaffolds or the effects of dynamic culture conditions in terms of cell proliferation, cell distribution, and osteogenic differentiation. In this study, particulate hES-MPs/coral and hMSCs/coral constructs were cultured in a packed bed/column bioreactor, which was designed for the culture of bone-engineered substitutes of clinical relevant volume. We hypothesized a beneficial effect of the 3D dynamic culture on hES-MPs and hMSCs, in terms of proliferation, osteogenic differentiation and tissue formation, and evaluated the potential of the investigated experimental approach for bone engineering applications.

Materials and Methods

Coral scaffolds

Three-dimensional scaffolds of natural coral (Porites species), with a dimension of about $3 \times 3 \times 3$ mm, were provided by Biocoral, Inc. (Inoteb). They consisted of calcium carbonate (98%–99%) in the form of aragonite with trace elements (0.5%–1%) and amino acids ($0.07\% \pm 0.02\%$). The volume porosity and the mean pore diameter were $49\% \pm 2\%$ and 250 μm (range 150–400 μm), respectively. All pores intercommunicated.[33] In Figure 1 a photograph (Fig. 1a) and a scanning electron microscope image (Fig. 1b) of the coral scaffold used are shown. Scaffolds were steam autoclaved at 115°C for 20 min, which was shown not to affect the composition.[34] Then, 330 coral scaffolds were washed three times (30 min) with Dulbecco's Modified Eagle Medium-High Glucose (DMEM-HG; PAA Laboratories) supplemented with 1% penicillin-streptomycin-amphotericin (PAA Laboratories). To remove air bubble entrapped within the material, samples were finally vacuum treated and incubated overnight at 37°C in 5% CO_2.

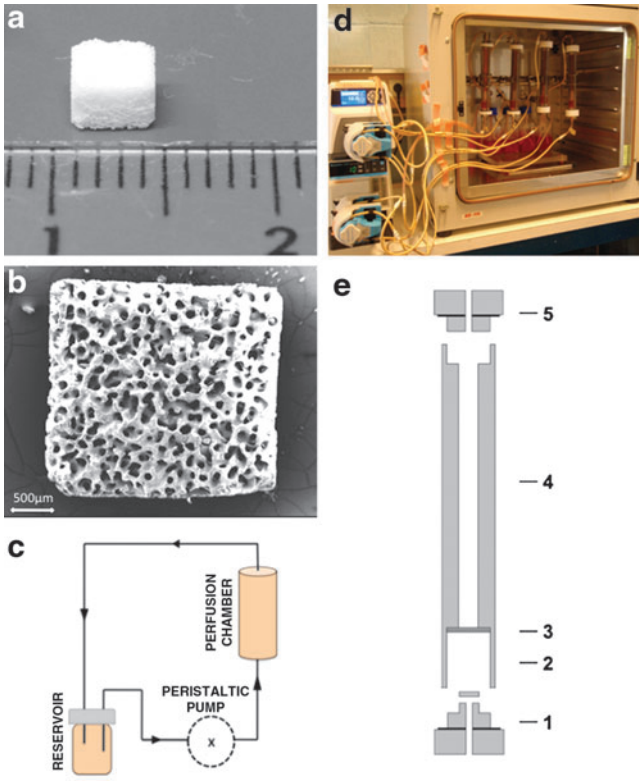

FIG. 1. Photograph **(a)** and SEM image **(b**; scale bar = 500 μm**)** of one of the coral scaffolds used in the study. Schematic illustration of the flow perfusion system **(c)**. Photograph of the flow perfusion bioreactor showing the peristaltic pumps and the perfusion chambers **(d)**. Schematic figure of the perfusion chamber of the packed bed/column bioreactor used in the present study **(e)**: bottom lid (1); entry chamber which serves to prevent fluid flow disturbances when medium from the reservoir enters the perfusion chamber (2); plastic grid with pores of 1 mm in diameter (3); perfusion chamber *per se* where scaffolds seeded with cells are cultured (inner diameter 12 mm) (4); upper lid (5). Color images available online at www.liebertpub.com/tea

Cell types

hMSCs were isolated after informed consent from bone marrow aspirates from the iliac crest of three patients (age 14, 27, and 43 years, respectively) undergoing spinal fusion. Briefly, 5 mL of fresh bone marrow was transferred into 5 mL of a solution of phosphate buffer containing Heparin E500 (Heparin LEO; Apoteket AB) to prevent coagulation. Adipose tissue was removed by centrifugation at 1800 rpm for 5 min. hMSCs were then isolated by gradient centrifugation using CPT Vacutainer® tubes prefilled with Ficoll (Pharmacia) according to manufacturer's instructions. The donation of bone marrow was approved by the ethics committee at the Medical Faculty at Gothenburg University (Dnr. 532-04). hMSCs were expanded in medium consisting of Dulbecco's Modified Eagle Medium-Low Glucose (DMEM-LG; PAA Laboratories) supplemented with 1% penicillin-streptomycin-amphotericin, L-glutamine (2 mM; Gibco), 10% fetal bovine serum (FBS; PAA Laboratories), and 10 ng/mL human recombinant beta-fibroblast growth factor (Invitrogen).

hES-MPs were provided by Cellartis (www.cellartis.com). The hES-MPs were derived from an undifferentiated hESC line (SA002.5), and the derivation and characterization of hES-MPs has been described earlier.[33,34] hES-MPs were expanded in DMEM-HG, supplemented with the same additives as described above for the hMSCs.

Media were changed every 3–4 days and cells were passaged when reaching about 80% confluence. Both cell types were cultured at 37°C in 5% CO_2.

Flow cytometry analysis

To verify enrichment of hMSCs, cells were stained with CD34-PerCP, CD45-FITC, CD105-FITC, and CD166-PE antibodies (all from Ancell). Samples were analyzed using the FACS Aria flow cytometer (Becton Dickinson AB) using the FACS Diva software (Becton Dickinson AB).

Cell seeding in scaffolds

Both cell types were treated with trypsin and seeded at a density of 10^5 cells per coral scaffold placed in 15 mL tubes. Briefly, cells were detached, filtered with 40 μm nylon strainers (BD Biosciences) to remove clusters of cells and counted. After centrifugation at 1200 rpm for 5 min, cells were resuspended in expansion medium consisting of DMEM-HG supplemented with the same additives as described above. To favor a homogenous distribution of cells across the scaffolds, tubes were gently shaken and tilted every 30 min for 4 h, and then incubated at 37°C in 5% CO_2 for 3 days before being transferred into flow perfusion bioreactors for osteogenic differentiation. Three days after seeding, the medium was collected and cells not attached to the corals counted in a hemocytometer to evaluate the degree of cell attachment.

Culture in packed bed/column bioreactor

Both hES-MP/coral and hMSC/coral constructs were transferred into four chambers (denoted day 0) of a packed bed/column bioreactor, whose description was previously reported,[35] and cultured for 5 weeks both in static (flow perfusion rate: 0 mL/min) and dynamic (flow perfusion rate: 10 mL/min; average shear stress estimated to be 0.001 Pa[36]) conditions [see Fig. 1 for a schematic illustration of the perfusion system (Fig. 1c), a photograph of the bioreactor with the incubated cell/coral constructs (Fig. 1d), and a diagram of an individual bioreactor chamber (Fig. 1e)]. This resulted in four groups of investigation denoted (1) hES-MPs static, (2) hES-MPs dynamic, (3) hMSCs static, and (4) hMSCs dynamic. Osteogenic medium consisted of DMEM-LG supplemented with HEPES (25 mM; Sigma), 1% penicillin-streptomycin-amphotericin, L-glutamine (2 mM), 10% FBS, L-ascorbic acid (4.5×10^{-5} M; Sigma), dexamethasone (10^{-6} M; Sigma), and β-glycerophosphate (2×10^{2} M; Calbiochem). Per each group 250 mL of medium were provided in the respective reservoir. All cells were incubated at 37°C. The medium was changed every 3–4 days and cell/coral constructs were harvested every week in order to examine cell proliferation and osteogenic differentiation. Medium samples were collected twice a week to assess pH, as well as glucose and lactate concentrations. No significant differences in these parameters were observed between all groups investigated along the entire experimental period (data not shown).

Fluorescein diacetate staining

To examine cell distribution across the coral scaffolds, three samples per each condition were collected at day 0 and weekly after incubation in bioreactor, and stained with fluorescein diacetate (FDA; Sigma). Samples were incubated 10 min at 37°C with the osteogenic medium supplemented with FDA at a final concentration of 0.1 μg/mL, and visualized under the fluorescence microscope Eclipse TE2000-U (Nikon).

Scanning electron microscopy

After 3 days and 5 weeks in bioreactors, cell/coral constructs were harvested for SEM characterization. Briefly, cell/coral constructs were rinsed twice in phosphate-buffered saline (PBS) before being fixed in a modified Karnovsky fixative, consisting of sodium azide (0.02%; Fluka Biochemika GmbH), paraformaldehyde (2%; Merk), and gluteraldehyde (2.5%; Fluka Biochemika) in sodium cacodylate buffer (0.05 M; Prolabo). Constructs were later treated with OsO_4 (1%; Agar Scientific) in sodium-cacodylate buffer, and stored at 4°C for 4 h. After rinsing five times with distilled H_2O, constructs were treated with hexamethyldisilazane (1%; Fluka, Sigma) before adding again a solution of OsO_4 (1%) in sodium cacodylate buffer (0.1 M). After dehydration with ethanol of increasing concentration (70%, 80%, 95%, and 99.5%), samples were treated twice (10 min) with hexamethyldisilazane (1%; Fluka, Sigma) and dried overnight. Then, all samples were sputter coated (EMITECH K550×; EMITECH) with palladium for 2 min at 25 mA before SEM examination. Native scaffolds were also SEM characterized following similar protocol. The SEM analysis was performed using a LEO Ultra 55 FEG SEM (Carl Zeiss AB) equipped with a secondary electron detector and an in-lens detector. Overview images were acquired using the secondary electron detector at 5 kVs acceleration voltage, whereas the in-lens detector was used for closer examination of the cell-scaffold interaction at 2 kVs acceleration voltage.

Total DNA content

Cell proliferation was investigated weekly by measuring the content of DNA. The total DNA content was

quantified using the Quant-iT™ PicoGreen® dsDNA reagent kits according to the manufacturer's instructions (Molecular Probes, Inc.). Cell/coral constructs were grinded frozen in liquid N_2 for 1 min at 30 Hz (Retsch). After the addition of 150 μL of Triton (0.1%; Sigma), three freeze–thaw cycles were performed. Then, 10 μL aliquots of lysed samples were incubated with 90 μL of 1×TE buffer and 100 μL of PicoGreen Working Reagent, and fluorescence was read using a fluorescence microplate reader with ex/em of 480/520 nm. A standard curve of known concentrations of λ DNA was used to convert fluorescence to total DNA content.

Total protein content

To quantify the deposited extracellular matrix, total protein content was measured using the BCA Protein Assay Reagent (Pierce Chemical Company) according to the manufacturer's instructions. Briefly, cell/coral constructs were grinded frozen in liquid N_2 for 1 min at 30 Hz (Retsch). After the addition of 150 μL of Triton (0,1%, Sigma), three freeze-thaw cycles were performed. A 10-μL aliquot of lysed samples was incubated for 30 min at 37°C with 200 μL of working reagent (mix of Cu and BCA in alkaline pH). Absorbance was read at 562 nm using the μQuant microplate reader (Bio-Tek Instruments). Protein concentration was determined using a standard curve of known concentrations of bovine serum albumin (Sigma).

Quantitative real-time PCR

Cell/coral constructs were harvested at day 0 and weekly after incubation in bioreactors for gene expression analysis. Samples were lysed in 1 mL of Trizol reagent (TRIzol® Reagent; Invitrogen) and total RNA was extracted according to the manufacturer's instructions. Briefly, samples were homogenized in the Trizol Reagent for 3 min at room temperature and vortexed three times for 20 s. About 400 μL of chloroform was added to each sample, and 500 μL of the aqueous phase containing RNA was collected. RNA was precipitated with isopropyl alcohol, washed in ethanol, and dissolved in RNase-free water. The purity and concentration of extracted RNA was measured with the spectrophotometer Nanodrop 1000 (Labtech). Reverse transcription was carried out in the iCycler thermal cycler (Bio-Rad Laboratories) using the SuperScript™ II Reverse Transcriptase Kit (Invitrogen) in a 20 μL volume reaction, according to the manufacturer's instructions. Real-time PCR was performed in triplicates using the MyiQTM Single-Color Real Time PCR (Bio-Rad Laboratories) in a 20-μL volume reaction containing equal volumes of cDNA, TaqMan Universal PCR Master Mix (Applied Biosystems) and TaqMan® Gene Expression Assays (Applied Biosystems) composed of FAM™ dye-labeled TaqMan MGB probe and predesigned unlabeled PCR primers for *RUNX2* (Hs00231692_m1), *COL1A1* (Hs00164004_m1), alkaline phosphatase (*ALPL*) (Hs01029144_m1), *OC* (Hs00609452_g1), *ON* (Hs00234160_m1), *OPN* (Hs00960942_m1), and 18S ribosomal subunit (Hs99999901_s1). Cycling conditions were 95°C for 10 min followed by 40 cycles of 95°C for 15 s (denaturation), 60°C for 60 s (annealing), and again 60°C for 60 s (extension). The fluorescence was read at the end of the extension step. The data were analyzed using MyiQ™ Software (Bio-Rad Laboratories), and the expression level of the gene of interest expressed as normalized for the expression level of the 18S ribosomal subunit.

Alkaline phosphatase activity

To investigate cell differentiation, intracellular ALP activity was measured weekly. ALP activity was assayed colorimetrically by using p-nitrophenylphosphate as substrate. Briefly, cell/coral constructs were grinded frozen in liquid N_2 for 1 min at 30 Hz (MM301; Retsh). After the addition of 150 μL of Triton (0.1%; Sigma), three freeze-thaw cycles were performed. Then, aliquots of cell extracts (50 μL) were incubated with 250 μL of 2-amino-2-methyl-propanol (pH 10.3; Sigma) and 250 μL of p-nitrophenylphosphate (15.2 mM; Sigma) in $MgCl_2$ (2 mM) at 37°C. The reaction was stopped adding 1 mL of NaOH (1 N). The quantity of p-nitrophenol produced was measured spectrophotometrically at 410 nm using the microplate reader μQuant (Bio-Tek Instruments), and was considered directly proportional to the ALP activity.

Histological analysis

After 5 weeks of culture under osteogenic conditions in bioreactor, cell/coral constructs were rinsed in PBS and fixed in 4% paraformaldehyde at 4°C for 24 h. Samples were decalcified in ethylenediaminetetraacetic acid (EDTA; pH 7) for 5 days, dehydrated in ethanol with increasing concentration and embedded in paraffin at Histocenter (Histocenter AB; www.histocenter.se). Four sections were cut from each sample, two at a depth of 20%–25% and two at a depth of 45%–50% of the cell/coral scaffold. Sections were then stained with hematoxylin-eosin-safranin (HES) and Syrius red[4] to investigate tissue formation and collagen deposition. The stained sections were observed with the light microscope Eclipse E600 (Nikon).

Time-of-flight secondary ion mass spectrometry

After 5 weeks of culture in bioreactors, cell/coral constructs were harvested for time-of-flight secondary ion mass spectrometry (TOF-SIMS) analyses. Briefly, samples were rinsed twice with PBS and fixed in 4% formaldehyde at 3°C–5°C. After fixation, samples were dehydrated in ethanol of increasing concentration, embedded in plastic resin (LR White; the London Resin Co Ltd.), and allowed to harden on ice. Then, each block was cut at a level corresponding to a depth of about 50% inward the cell/coral construct using the Exakt cutting-grinding equipment (EXACT Technologies, Inc.). For TOF-SIMS analysis, samples were mounted on a sample holder allowing for imaging mass spectrometry analysis of cross sections of the cell/coral construct. Two samples each of the four different groups were analyzed by TOF-SIMS.

TOF-SIMS analysis was carried out using a TOF-SIMS IV instrument (IONTOF Technologies GmbH) equipped with a Bi_n^+ cluster primary ion source and a C_{60}^+ ion source for sputtering. Before each analysis, the sample surface was sputter cleaned using 10 keV C_{60}^+ ions over an area of $600 \times 600\ \mu m^2$ for 200 s at a C_{60}^+ current of 0.3 nA. TOF-SIMS data were acquired using 25 keV Bi_3^+ primary ions with the instrument optimized either for high mass resolution (bunched mode, mass resolution $m/\Delta m \sim 7000$, lateral resolution $\Delta l \sim 3$–$5\ \mu m$) or for high image resolution (BA mode, $m/\Delta m$

Table 1. Characteristic Ions Used for TOF-SIMS Imaging of the Cell/Scaffold Constructs

Fragment ion	*m/z*	*Origin*	*Bunched/BA*
CH_3O^+	31.02	Resin	bu/BA
$C_2H_3O^+$	43.02	Resin	bu
$C_4H_7^+$	55.06	Resin	BA
$C_4H_5O^+$	69.04	Resin	bu/BA
$C_7H_7^+$	91.06	Resin	BA
$CaPO_2^+$	102.93	Calcium phosphate	bu
$Ca_2PO_3^+$	158.89	Calcium phosphate	bu/BA
$Ca_2PO_4^+$	174.88	Calcium phosphate	bu/BA
$Ca_3PO_4^+$	214.84	Calcium phosphate	bu/BA
$Ca_3PO_5^+$	230.84	Calcium phosphate	bu/BA
$Ca_4PO_6^+$	286.79	Calcium phosphate	bu/BA
$(CaO)_3H^+$	168.88	Calcium carbonate	bu/BA
$(CaO)_4H^+$	224.84	Calcium carbonate	bu/BA
$(CaO)_5H^+$	280.79	Calcium carbonate	bu/BA
$(CaO)_6H^+$	336.75	Calcium carbonate	bu/BA

TOF-SIMS, time-of-flight secondary ion mass spectrometry.

$\sim$300, Δl $\sim$200 nm). Spectra and ion images were recorded in the bunched mode over an analysis area of $500\times500\,\mu m^2$ (256×256 pixels) for 200 s at a pulsed primary ion current of 0.1 pA and over an analysis area of $150\times150\,\mu m^2$ (256×256 pixels) at a pulsed primary ion current of 0.04 pA for 300 s in the burst alignment mode. For each sample, three areas were analyzed in the bunched mode, and among those a smaller area was selected for high image resolution analysis (BA mode). Ion images showing the localization of the three different components of the sample (calcium carbonate, calcium phosphate, and resin) were obtained by adding the signal from several characteristic ions for each component, as specified in Table 1. The reason for using slightly different peaks in the bunched and BA modes is the higher mass resolution in the bunched mode, which allows for better selection of characteristic ions without interference with other ions.

Statistical analyses

Results are expressed as means and standard deviations. Differences were determined by the nonparametric Mann–Whitney test for independent samples using SPSS Statistics 17.0 software. For all the analyses, a value of $p\leq0.05$ was considered as significant difference. Three to six samples were used per each analysis.

Results

Flow cytometry analysis of hMSCs

Flow cytometry analysis was used to evaluate the enrichment of a homogenous population of hMSCs. Our results demonstrate that 96%±2% of the cells were CD166+/CD45− and 94%±1% of the cells were CD105+/CD34− (data not shown). Only hMSCs from the 14-year-old donor were evaluated in flow perfusion bioreactor, due to their higher osteogenic potential as reported previously.[32]

Cell attachment and distribution

The efficiency of cell attachment to the coral scaffolds was assessed by counting the nonattached cells in collected medium at day 0 (i.e., 3 days after seeding and before the transfer of tissue construct into bioreactor), resulting in a seeding efficiency higher than 98% for both cell types (data not shown). In Figure 2a and b, FDA-stained cell/coral constructs before culture in bioreactor are shown. Constructs, either seeded with hES-MPs (Fig. 2a) or hMSCs (Fig. 2b), display a homogenous distribution of cells across the scaffold surface. Cell attachment to the coral scaffolds was confirmed by SEM analysis 3 days after culture in bioreactor as shown in Figure 2c–f. A cellular layer covering the coral scaffold surface is observed for both hES-MPs (Fig. 2c, e) and hMSCs (Fig. 2d, f) under static (Fig. 2c, d) and dynamic (Fig. 2e, f) conditions. Except occasional side-to-side variations, a homogenous cell distribution across the scaffolds was seen along the entire duration of the experiment by microscopic observation (data not shown).

Cell proliferation and protein content

The effect of dynamic conditions on cell proliferation was investigated by measuring the DNA and protein content at day 0 and weekly after culture in bioreactors. In Figure 3a, the DNA content of coral scaffolds seeded with hES-MPs or hMSCs and cultured either under static or dynamic conditions is shown. At day 0, a significant difference in DNA

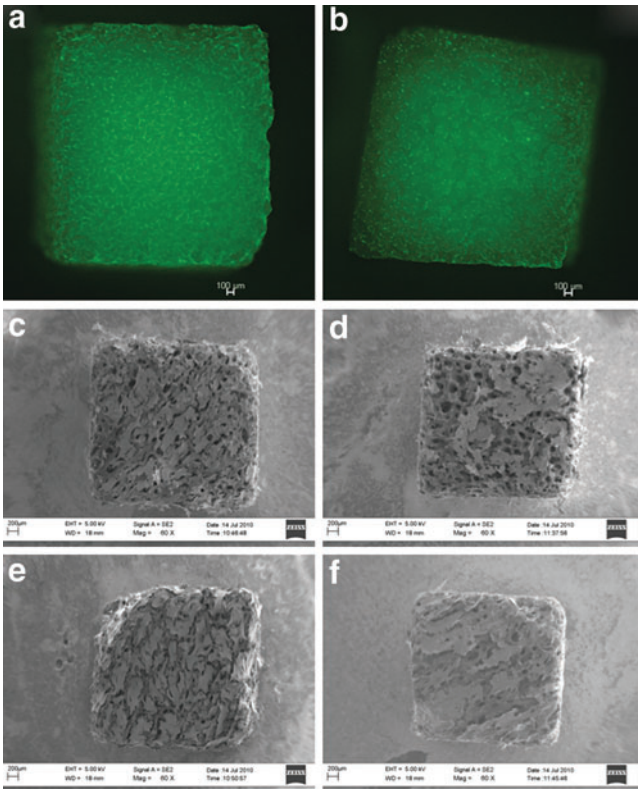

FIG. 2. Fluorescent microscope pictures of fluorescein diacetate-stained cell/coral constructs, showing cell distribution of human embryonic stem cell-derived mesodermal progenitor (hES-MPs) **(a)** and human mesenchymal stem cells (hMSCs) **(b)**, before incubation into bioreactor; scale bar = 100 μm. SEM images of cell/coral constructs after 3 days of culture in bioreactor for hES-MPs **(c, e)** and hMSCs **(d, f)** under static **(c, d)** and dynamic **(e, f)** conditions respectively; scale bar = 200 μm. Color images available online at www.liebertpub.com/tea

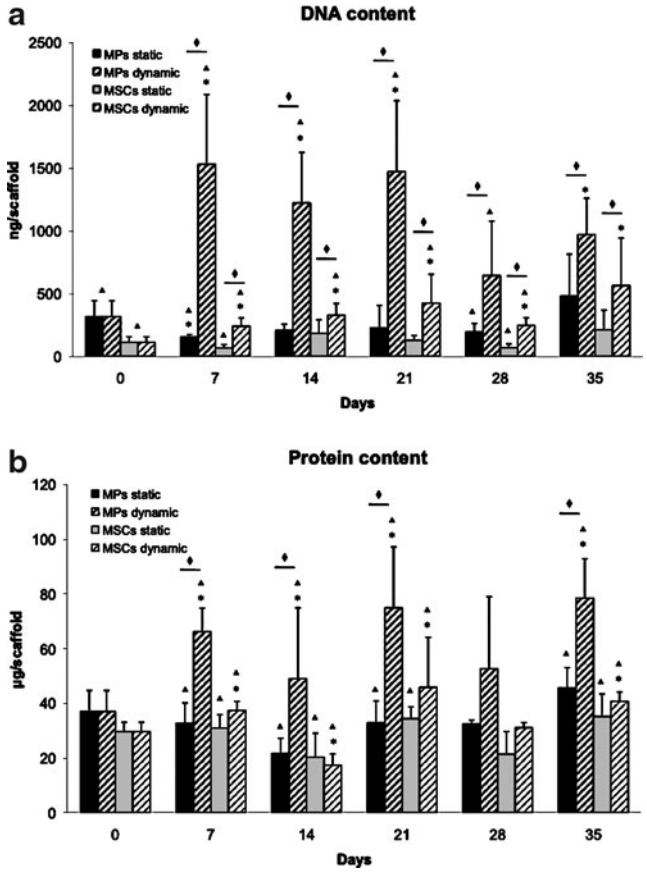

FIG. 3. Graphs displaying the total DNA **(a)** and protein **(b)** contents along the entire duration of the experiment for hES-MPs (MPs) and hMSCs (MSCs) under static and dynamic conditions. A value of $p < 0.05$ was taken as significant difference (* denotes significant differences over day 0; ◆ denotes significant differences between culture conditions; ▲ denotes significant differences between cell types under similar conditions).

content was observed between constructs of hES-MPs and hMSCs, with constructs of hES-MPs showing a 2.8-fold higher DNA content than constructs of hMSCs. When cultured under static conditions, both constructs of hES-MPs and hMSCs did not display any significant increase in DNA content compared to the respective content at day 0. On the other hand, when cultured under dynamic conditions, both constructs of hES-MPs and hMSCs displayed significant increase in DNA content compared to the respective content at day 0, as well as the content observed when cultured under static conditions. However, under dynamic conditions the DNA content for constructs of hES-MPs was significantly higher than the content observed for constructs of hMSCs along all the experimental period.

Likewise the increase in DNA content detected, a higher protein content was observed when constructs were cultured under dynamic conditions as shown in Figure 3b. Both constructs cultured under dynamic conditions displayed a significant increase in protein content after 7, 14, 21, and 35 days compared to the respective content observed at day 0. Noteworthy, at each time point investigated (except for day 28), the protein content for constructs of hES-MPs cultured under dynamic conditions was significantly higher than the content observed for constructs of hMSCs cultured under the same conditions. On the other hand, no significant variations were found when constructs were cultured under static conditions for both cell types, although a significantly higher protein content was observed for constructs of hES-MPs compared to hMSCs after 35 days of culture.

Gene expression

Expression of markers involved in osteogenic differentiation was evaluated by real-time PCR and the results were normalized to the expression of the ribosomal unit 18S. In Figure 4a the expression of *RUNX2* is shown. At day 0, the expression level of *RUNX2* was significantly higher for constructs of hES-MPs compared to hMSCs. Constructs of hES-MPs cultured under static conditions displayed a significant increase in *RUNX2* expression at day 7 and 28 compared to day 0. Under dynamic conditions instead, after a significant increase in expression observed at day 7, the expression level decreased at day 14, and then increased again and remained significantly higher at days 21, 28, and 35. In a different fashion, constructs of hMSCs showed a significantly increased expression of *RUNX2* at all time points investigated compared to day 0, both when cultured under dynamic and static conditions. Besides the differences in expression profile observed for constructs of hES-MPs and hMSCs, from week 2 onward *RUNX2* expression appeared to be significantly higher for constructs of hMSCs compared to hES-MPs, both under static conditions at day 14 and 21 and dynamic conditions at day 14, 28, and 35.

The expression levels of *COL1A1* are shown in Figure 4b. At day 0, the expression of *COL1A1* for constructs of hES-MPs was about 4-fold higher than for constructs of hMSCs. After incubation, constructs of hES-MPs cultured under dynamic conditions displayed a significantly increased expression of *COL1A1* at day 21 and 28. On the other hand, when the same constructs were cultured under static conditions, a significant decrease in *COL1A1* expression was observed during the first 2 weeks of culture, followed by a significant increase at day 28 and 35. hMSCs instead displayed a significant increased expression of *COL1A1* at all time points investigated when cultured under dynamic conditions, while no general variations in expression were observed at day 7, 14, 21, and 35 under static conditions. Although the overtime increase observed for constructs of hMSCs, the expression of *COL1A1* was generally higher for constructs of hES-MPs along the experimental period under both culture conditions. The expression results for *ALPL* are shown in Figure 4c. Constructs of hES-MPs, under both conditions, displayed a progressive increase in the expression of *ALPL* from day 14 onward, although the observed increase was found to be significantly higher when constructs were cultured under dynamic conditions. A different profile was observed for constructs of hMSCs. In static conditions the expression level of *ALPL* was significantly higher at each time point investigated, while a gradual increase along the experimental period was observed when the constructs were cultured under dynamic conditions. Under static conditions, the *ALPL* expression was significantly higher for constructs of hMSCs compared to hES-MPs, whereas an opposite trend was observed under dynamic conditions.

The expression level of *OC* at day 0 was significantly higher for constructs of hMSCs compared to constructs of

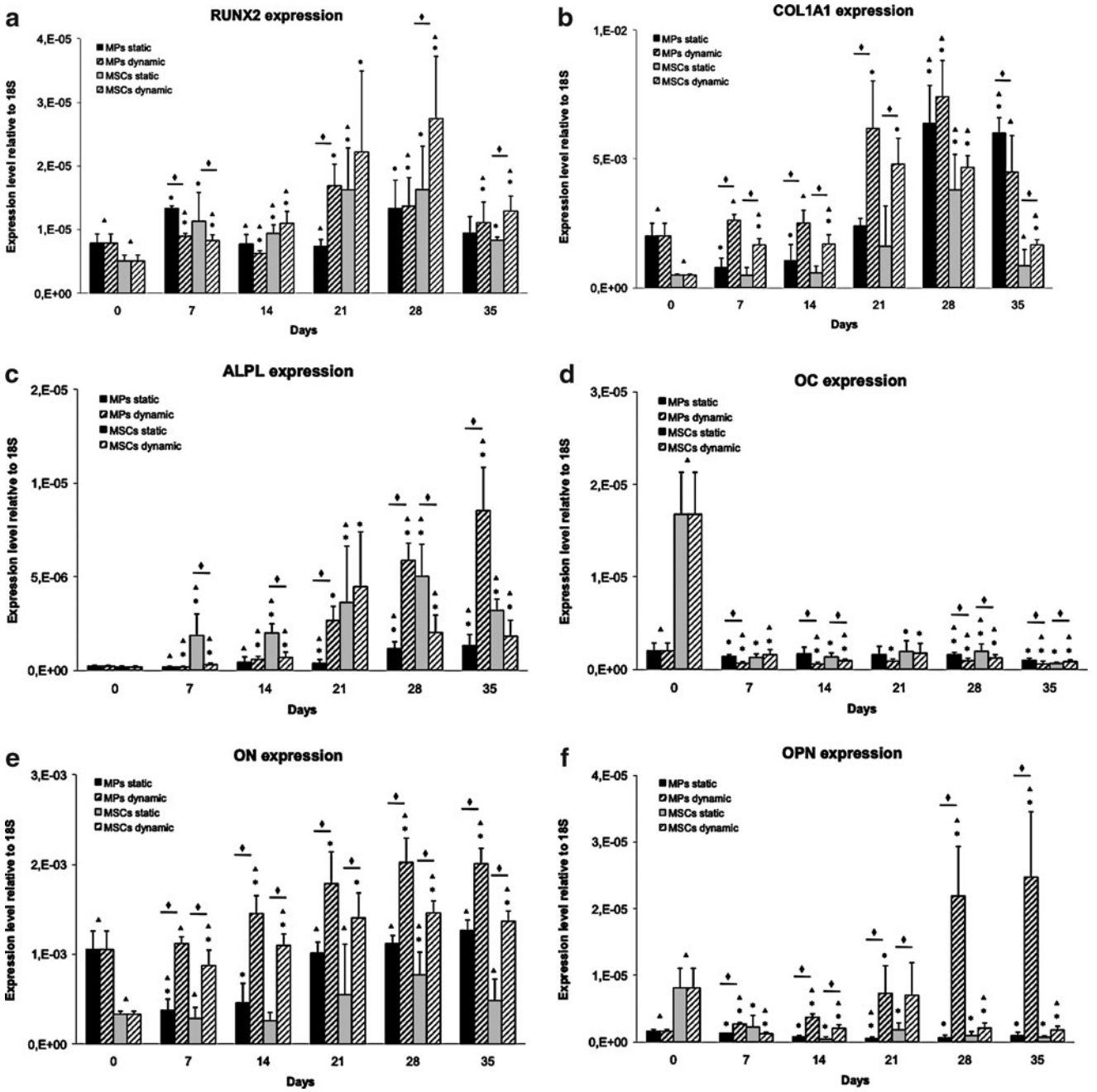

FIG. 4. Real-time PCR results showing expression level of *RUNX2* **(a)**, *COL1A1* **(b)**, alkaline phosphatase (*ALPL*) **(c)**, *OC* **(d)**, *ON* **(e)**, and *OPN* **(f)** for hES-MPs (MPs) and hMSCs (MSCs) cultured under static and dynamic conditions. A value of $p < 0.05$ was taken as significant difference (* denotes significant differences over day 0; ◆ denotes significant difference between culture conditions; ▲ denotes significant differences between cell types under similar conditions).

hES-MPs as shown in Figure 4d. However, after stimulation, all constructs displayed a decreased expression of *OC*, especially when cultured under dynamic conditions.

An opposite trend was observed when analyzing the expression level of *ON*. At day 0, in fact, the expression level of *ON* was significantly higher for constructs of hES-MPs compared to constructs of hMSCs as shown in Figure 4e. After flow perfusion, both constructs displayed increased expression of *ON* at all time points investigated, while no substantial increase was observed when constructs were cultured under static conditions. Despite the similar trend observed, constructs of hES-MPs displayed a significantly higher *ON* expression along the experimental period, both under static conditions and dynamic conditions.

A distinct expression profile was found when studying the expression of *OPN* as shown in Figure 4f. At day 0, the expression level was higher for constructs of hMSCs compared to constructs of hES-MPs. However, under dynamic conditions, constructs of hES-MPs displayed a significant increase in *OPN* expression along the experimental period.

ALP activity

The effect of dynamic conditions in modulating osteogenic differentiation was also investigated by measuring the ALP activity weekly. The data in Figure 5 demonstrate that at day 0 the ALP activity was significantly lower for constructs of hES-MPs compared to hMSCs. When cultured either under static or dynamic conditions, both constructs of hES-MPs and hMSCs displayed a gradual increase in ALP activity along the experimental period. Noteworthy, the static conditions were generally associated with a higher ALP activity for both constructs. However, constructs of hES-MPs displayed a significant higher ALP activity under dynamic condition compared to static conditions after 35 days. Overall, the ALP activity was higher for constructs of hMSCs compared to hES-MPs up to 28 days. On the other hand, an opposite trend was observed after 35 days, with constructs of hES-MPs displaying significantly higher ALP activity compared to constructs of hMSCs under both conditions.

Tissue development

Histological staining was used to study tissue formation. In Figure 6a–h, HES-stained sections of decalcified cell/coral constructs are shown. Coral scaffolds seeded with hES-MPs (Fig. 6a–d) displayed a stark increase in cellular growth and tissue formation when cultured under dynamic conditions (Fig. 6c, d) compared to static conditions (Fig. 6a, b). Interestingly, for both conditions, constructs of hES-MPs showed an increased area of formed tissue compared to hMSCs (Fig. 6e–h). Although coral scaffolds seeded with hMSCs and cultured under dynamic conditions (Fig. 6g, h) appeared to display a denser tissue formation compared to static conditions (Fig. 6e, f), no differences were observed in the area of formed tissue. The increased tissue development observed for constructs of hES-MPs cultured under dynamic conditions was associated with deposition of a dense network of collagen fibers as shown in Figure 6i and j. Less intense coloration was observed for all the other investigated conditions (data not shown). Displayed results correspond to sections cut at a depth of 45%–50% inside the constructs. Similar patterns were observed for sections cut at a depth of 20%–25% inside the constructs (data not shown).

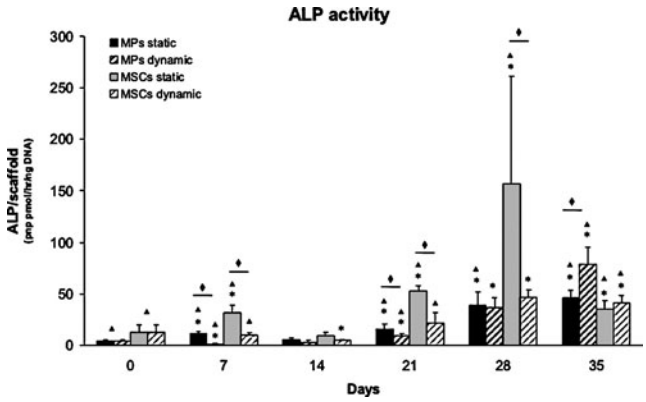

FIG. 5. Graph displaying the ALP activity for constructs of hES-MPs (MPs) and hMSCs (MSCs) cultured under static and dynamic conditions. A value of $p < 0.05$ was taken as significant difference (* denotes significant differences over day 0; ◆ denotes significant difference between culture conditions; ▲ denotes significant differences between cell types under similar conditions). Results are expressed as normalized per content of DNA.

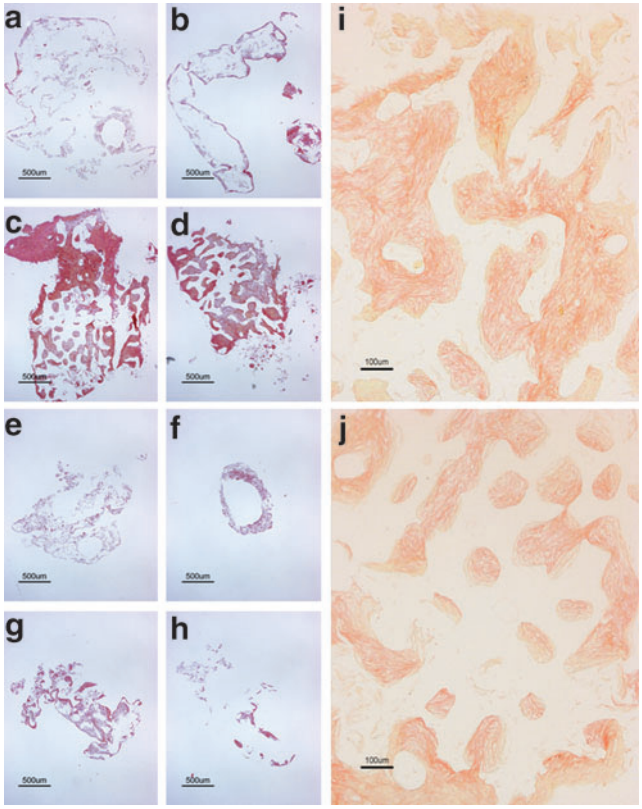

FIG. 6. Histological micrographs of construct seeded with hES-MPs and hMSCs after 5 weeks of culture. Hematoxylin-eosin-saffanin (HES)-stained sections of hES-MPs cultured under static **(a, b)** and dynamic conditions **(c, d)**. HES-stained sections of hMSCs cultured under static **(e, f)** and dynamic conditions **(g, h)**; scale bar = 500 μm. Sirius red-stained sections of hES-MPs cultured under dynamic conditions **(i, j)**; scale bar = 100 μm. Color images available online at www.liebertpub.com/tea

Calcium phosphate deposition

In Figure 7, TOF-SIMS three-color overlay images of cell/coral constructs are shown. Interestingly, it appears that the dynamic conditions favor the deposition of calcium phosphate minerals (green) for both cell/coral constructs, either seeded with hES-MPs (Fig. 7e–h) and hMSCs (Fig. 7m–p), especially considering the central regions of the constructs (Fig. 7e and h, respectively), as opposed to static conditions, where poor mineralization was observed for both constructs of hES-MPs (Fig. 7d) and hMSCs (Fig. 7l). Scaffolds seeded with hMSCs and cultured under static conditions displayed poor mineralization also across the construct periphery as shown in Figure 7i–k. Interestingly, for all conditions investigated, mineralization takes generally place at the interface with the coral scaffold (blue). However, constructs of hES-MPs cultured under dynamic conditions appeared to display areas of mineralization also further down inside the scaffold pores as shown in Figure 7e.

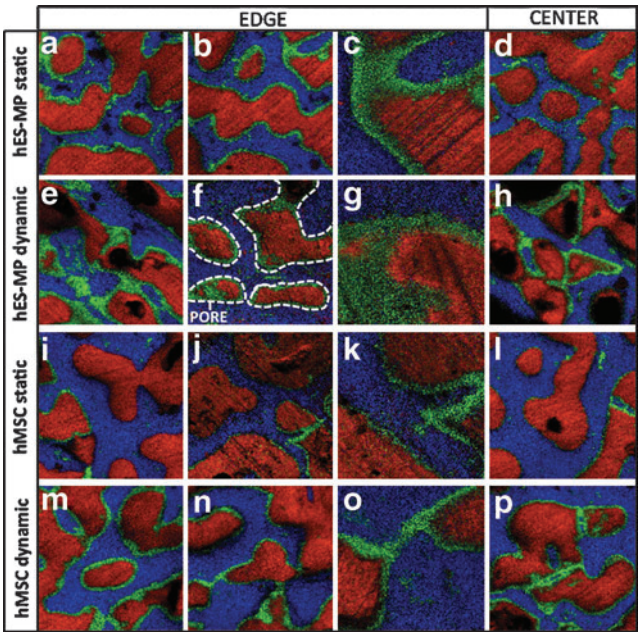

FIG. 7. Three-color overlay TOF-SIMS images showing the two-dimensional distribution of resin (red), calcium phosphate (green), and coral (blue). Images of hES-MPs/coral constructs cultured under static [**(a, b, d):** field of view = $500 \times 500\,\mu m$; **(c):** field of view = $150 \times 150\,\mu m$] and dynamic conditions [**(e, f, h):** field of view = $500 \times 500\,\mu m$; **(g):** field of view = $150 \times 150\,\mu m$]. Images of hMSCs/coral constructs cultured under static [**(i, j, l):** field of view = $500 \times 500\,\mu m$; **(k):** field of view = $150 \times 150\,\mu m$] and dynamic conditions [**(m, n, p):** field of view = $500 \times 500\,\mu m$; **(o):** field of view = $150 \times 150\,\mu m$]. Pores are indicated by the dotted line. Color images available online at www.liebertpub.com/tea

Discussion

In bone engineering, the development of dynamic culture strategies is emerging as an essential aspect to improve proliferation and differentiation of the cells in the scaffold by enabling nutrient supply, providing mechanical stimulation and a proper environment for the reproducible and large-scale production of the engineered tissues. Several authors have recently reported encouraging results after culturing tissue-engineered constructs of hMSCs in various bioreactor systems, demonstrating increased cell proliferation[10,37] and osteogenic differentiation.[10,11,38–40] In this study we report the beneficial effects of dynamic culture conditions provided by a packed bed/column bioreactor on hES-MPs, which results in significantly increased bone-like tissue formation compared to hMSCs. Cells were interfaced to small coral particles of cuboid shape and cell/coral constructs cultured in a packed bed/column bioreactor. This type of bioreactor was chosen for the current study because of its high potential for application in clinical situation where the size of the patients' defects is highly variable. It is designed to accommodate up to 200 standardized cell/scaffold constructs (each of $\sim 3\,mm^3$) that could be used to reconstruct clinically relevant bone defects of any shape.[35] The empty spaces in between the small-sized cell/scaffold constructs in the bed/column bioreactor used in this study allow flow perfusion without significant resistance to the flow overtime. The osteogenic potential of bone constructs engineered using this type of bioreactor was proved *in vivo* when implanted subcutaneously in sheep.[35] Particularly relevant to the production of bioengineered bone in a clinical setting, custom-made bone constructs could be produced using such perfusion bioreactor, where each chamber is designed to accommodate about $20\,cm^3$ of cell/scaffold constructs.

Our data demonstrate that dynamic culture of both hES-MPs and hMSCs constructs in a packed bed/column bioreactor significantly promote cell proliferation, as indicated by the general increase in DNA and protein content observed, which is in accordance with data reported by other groups culturing hMSCs under dynamic conditions in bioreactor systems.[37,41] Perfusion of culture medium is recognized to affect cell proliferation through two main mechanisms, specifically by enabling mass transport and exerting fluid-driven mechanical stimulation,[42,43] but no clear data exist today concerning the independent role of the above mechanisms in promoting cell proliferation. The increased cell proliferation observed is likely due to the increase in nutrient transport and local O_2 tension associated with flow perfusion, which are recognized to promote hMSCs proliferation.[44] Moreover, the observed increase in proliferation may be dependent on the shear stress associated with flow perfusion, which has been reported to influence cell proliferation through multiple interacting and competing signal transduction pathways.[51] However, no progressive increase was observed over time for all conditions investigated. This may be because DNA cannot be easily released when cells are embedded in a mineralized matrix as previously proposed,[13,45] or possibly reflect a stable balance between cell proliferation and cell death. For example, Lynch *et al.* reported evidences that cells undergo programmed cell death upon osteogenic differentiation and development of bone-like tissue formation *in vitro*.[46] Nevertheless, at this moment it is not clear whether the increased DNA content observed for constructs cultured under dynamic conditions is due to an actual increased proliferation or reduced cell death, and further experiments aimed at investigating the cellular live-dead ratio within the constructs are needed.

Histological analysis of paraffin-embedded cell/coral constructs corroborated the DNA and protein data, especially with regard to constructs of hES-MPs cultured under dynamic conditions, where a stark increase in tissue formation was observed both in terms of density and area of formed tissue. The sharp dissimilarity in tissue formation observed between constructs of hES-MPs and hMSCs cultured under dynamic conditions is likely to be associated with the higher DNA content observed within constructs of hES-MPs at day 0, as well along the entire duration of the experimental period, which reflects the superior proliferation ability of hES-MPs compared to hMSCs.[31] Alternatively, a possible explanation for this finding may be the higher expression of the epithelial growth factor receptor (EGFR) observed in undifferentiated hES-MPs,[31] which was recently demonstrated to be activated after mechanical stimulation of the cells.[47]

The effect of dynamic culture conditions on cell differentiation was also investigated by studying the expression of genes involved in osteogenic differentiation and characteristic of the extracellular matrix of bone tissue. In our study the perfusion load was associated with a diminished expression of *RUNX2* during the early stage of culture

compared to static conditions, as recently reported by other authors,[11] but appeared to promote *RUNX2* expression at later time points, both for constructs of hES-MPs and hMSCs. Accordingly, the expression level of *COL1A1*, whose expression is induced by *RUNX2*,[48] was found to be significantly higher when constructs of hMSCs were cultured under dynamic conditions, specifically at later time points. The higher *RUNX2* and *COL1A1* expression, observed at day 0 for constructs of hES-MPs, is not consistent with our previous study,[36] and may be attributable to intrinsic properties of the coral scaffold used in this study,[49] including geometrical, chemical, and topographic features. Although the many-fold increase observed when constructs of hMSCs were cultured under dynamic conditions, the expression of *COL1A1* was typically higher in hES-MPs. The higher *COL1A1* expression together with the higher cellularity observed for constructs of hES-MPs under dynamic conditions explain the large differences found in the amount of collagen fibers deposited within the constructs, as indicated by the denser network of collagen fibers observed after staining with Red Sirius.

ALPL plays an important role in the early phases of mineralization of newly formed bone and the ALP activity is largely used as marker of osteogenic differentiation.[50] In our study the expression of *ALPL* in constructs of hES-MPs displayed a significant increase when constructs were cultured under dynamic conditions, suggesting a strong synergistic effect exerted by the combination of osteogenic factors and perfusion stimulation in promoting osteogenic differentiation. Interestingly, the increase in *ALPL* expression was found to correlate with the ALP activity results, although slightly different correlations were found when constructs were cultured under static and dynamic conditions. In fact, the increase in ALP activity was higher for constructs cultured under static conditions compared to dynamic conditions, with respect to the corresponding levels of *ALPL* expression. The difference in correlation observed may in part be due to technical limitations and in part to complex biological factors underlying gene expression and protein biosynthesis.[51] Otherwise, the discrepancy observed between ALP expression and activity under dynamic conditions may result from a washout effect associated with the flow. In fact, ALP exists both as membrane-bound and released enzyme, and the dynamic conditions may contribute to remove the released isoform from the constructs and lead to underestimation of its activity.[52] In relation to this, the authors strongly suggest to consider such a possibility in future studies using 3D scaffolds cultured under dynamic conditions. Dissimilar *ALPL* expression profiles were instead found for constructs of hMSCs, where the dynamic conditions were associated with a lower level of *ALPL* expression, underscoring a different responsiveness of hMSCs to the mechanical stimulation compared to hES-MPs. In accordance with gene expression results, the ALP activity was generally higher when constructs of hMSCs were cultured under static conditions, indicating a negative effect exerted by the flow perfusion on ALP activity.

Osteogenic differentiation was also assessed by investigating the expression of genes encoding for noncollagenous proteins, which are known to play a role in the mineralization of the extracellular matrix of bone tissue.[53] In our study, despite the large differences observed at day 0, both constructs of hES-MPs and hMSCs displayed a significant decrease in expression of *OC* gene after stimulation. The finding is not in agreement with the significantly increased expression observed for *RUNX2*, and may be dependent on other factors involved in the regulation of *OC* expression, such as for example the AP-1-related protein.[54,55] Noteworthy, the dynamic conditions were associated with a further downregulation of *OC* expression both for constructs of hES-MPs and hMSCs. Similar results were previously reported by others,[11,41] demonstrating that hMSCs underwent a significant decrease in expression of *OC* when cultured under dynamic conditions. The mechanical stresses associated with the dynamic conditions may account for the *OC* downregulation observed, and different perfusion loads may result more optimal in stimulating the expression of *OC*. However, Ducy *et al.* demonstrated that *OC*-deficient mice displayed increased bone formation and mineralization, indicating that a low expression of *OC* gene may be desirable when engineering bone tissue and not affect the construction of functional substitutes.[56] Interestingly, we recently demonstrated that, after protracted expansion, both hES-MPs and hMSCs displayed a significant increase in *OC* expression, and the *OC* upregulation was associated with limited matrix mineralization.[31,32]

In a different fashion, we found that both constructs of hES-MPs and hMSCs cultured under dynamic conditions displayed a significantly increased expression of *ON* compared the expression level observed at 0, and in all cases significantly higher than the corresponding values observed when the constructs were cultured under static conditions, suggesting that diverse biological components govern the expression of genes encoding noncollageneous proteins. The beneficial effect of flow perfusion on *OPN* expression was recently reported by other groups using human fetal bone cells and immortalized human bone marrow cells.[11,57] In contrast, our study demonstrated a decrease in *OPN* expression after culturing constructs of hMSCs under both static and dynamic conditions, although the dynamic conditions appeared to significantly stimulate the expression of *OPN* compared to static conditions after 14 and 21 days. In this regard, Scaglione *et al.* demonstrated that, in 2D systems, the changes in *OPN* and other bone salioprotein expression in response to flow were dependent on the substrate used,[58] suggesting that the properties of the biomaterial used in this study may account for the absent increase in *OPN* expression observed. On the other hand, the absent responsiveness observed for constructs of hMSCs may reflect the heterogeneous phenotype and biological functionality of osteoblastic cells, which has been reported to be associated with a rather variable pattern of gene expression.[59] Differently, the dynamic conditions were found to be associated with a significant increased expression of *OPN* for constructs of hES-MPs, highlighting the complex biology underlying cell differentiation, and demonstrating that different cell types may undertake distinctive biological pathways during lineage specification.

Both constructs of hES-MPs and hMSCs in all conditions investigated, regardless the differences observed in the expression of genes involved in osteogenic differentiation, displayed deposition of calcium phosphate minerals within the synthesized extracellular matrix. In this study the quantification of calcium, which is the usual procedure to

investigate matrix mineralization, was not possible by conventional methods due to the presence of calcium ions within the coral scaffolds. Therefore, a TOF-SIMS analysis of the resin-embedded samples was performed. TOF-SIMS has lately been exploited for examination of matrix mineralization after osteogenic differentiation.[22,32,60,61] Interestingly, in all conditions investigated, mineralization appeared to take place preferably at the interface with the coral scaffold, where a layer of calcium phosphate minerals deposited along the coral scaffold surface was observed. In fact, cells initially tend to populate the coral surface that functions as scaffold material for cell attachment and proliferation. Upon differentiation, cells start laying the extracellular matrix that eventually mineralizes. We recently reported that in monolayer cultures of hMSCs and hES-MPs mineral deposition occurred mainly at the interface with the substrate, beneath a superposed layer of synthesized extracellular matrix.[32] However, constructs of hES-MPs cultured under dynamic conditions appeared to deposit nodules of calcium phosphate further down inside the scaffold pores. After proliferation, additional layers of cells are expected to pile up with concomitant synthesis of extracellular matrix and subsequent deposition of calcium phosphate minerals. In this view, the more extensive areas of mineralized matrix seen for constructs of hES-MPs cultured under dynamic conditions possibly reflect the higher cellularity and denser extracellular matrix observed for these constructs, as well as the higher expression of genes involved in osteogenic differentiation, including *COL1A1*, *ON,* and *OPN*.

Taken together, the reported results demonstrate that the dynamic conditions provided by the packed bed/column bioreactor used in this study strongly promote cell proliferation, osteogenic differentiation, and bone-like tissue development of hES-MPs. Especially considering the stark increase in tissue formation and matrix deposition compared to hMSCs, hES-MPs represent a compelling alternative cell source for the fabrication of bone-engineered constructs for the repair of skeletal defects. However, it is important to note that additional studies aimed at investigating the independent role of mass transport and shear stress, as well as finding more specific conditions, are fundamental to define the optimal parameters for the successful culture of functional hES-MPs/scaffold constructs for applications in clinical settings.

Conclusions

The use of bioreactors in bone engineering applications is fundamental for the fabrication of 3D cell/scaffold constructs, for they promote cell proliferation and drive osteogenic differentiation. Moreover, the choice of an optimal cell source is of great importance for the rapid and effective fabrication of functional bone substitutes. Our study demonstrates that hES-MPs, when cultured under dynamic conditions in a packed bed/column bioreactor, display significantly increased cellularity, extracellular matrix production, and bone-like tissue development compared to hMSCs, suggesting that pluripotent stem cell derived-mesodermal progenitors may represent an interesting cell source for the fabrication of bone substitutes for the repair of large skeletal defects in humans.

Acknowledgments

We sincerely thank Helena Brisby for providing bone marrow samples and Lena Emanuelsson for helping with histology. We acknowledge BIOMATCELL VINN Excellence Center of Biomaterials and Cell Therapy, Region Västra Götaland, Swedish Research Council (K2009-52X-09495-22-3 and 2005-7544), JOIN(ed)T Marie Curie Action and the Centre National de la Recherche Scientifique for the financial support of the study.

Disclosure Statement

No competing financial interests exist.

References

1. Mikos, A.G., Herring, S.W., Ochareon, P., Elisseeff, J., Lu, H.H., Kandel, R., Schoen, F.J., Toner, M., Mooney, D., Atala, A., Van Dyke, M.E,, Kaplan, D., and Vunjak-Novakovic, G. Engineering complex tissues. Tissue Eng **12,** 2006.
2. Bilodeau, K., and Mantovani, D. Bioreactors for tissue engineering: focus on mechanical constraints. A Comparative Review. Tissue Eng **12,** 2006.
3. Martin, I., Wendt, D., and Heberer, M. The role of bioreactors in tissue engineering. Trends Biotechnol **22,** 2004.
4. El Haj, A.J., and Cartmell, S.H. Bioreactors for bone tissue engineering. Proc Inst Mech Eng H **224,** 2010.
5. Tapp, H., Hanley, E.N., Jr., Patt, J.C., and Gruber, H.E. Adipose-derived stem cells: characterization and current application in orthopaedic tissue repair. Exp Biol Med (Maywood) **234,** 2009.
6. Matsumoto, T., Kuroda, R., Mifune, Y., Kawamoto, A., Shoji, T., Miwa, M., Asahara, T., and Kurosaka, M. Circulating endothelial/skeletal progenitor cells for bone regeneration and healing. Bone **43,** 2008.
7. Jager, M., Zilkens, C., Bittersohl, B., and Krauspe, R. Cord blood-an alternative source for bone regeneration. Stem Cell Rev Rep **5,** 2009.
8. Danisovic, L., Varga, I., Polak, S., Ulicna, M., Bohmer, D., and Vojtassak, J. Morphology of in vitro expanded human muscle-derived stem cells. Biomed Pap Med Fac Univ Palacky Olomouc Czech Repub **152,** 2008.
9. Pittenger, M.F., Mackay, A.M., Beck, S.C., Jaiswal, R.K., Douglas, R., Mosca, J.D., Moorman, M.A., Simonetti, D.W., Craig, S., and Marshak, D.R. Multilineage potential of adult human mesenchymal stem cells. Science **284,** 1999.
10. Grayson, W.L., Frohlich, M., Yeager, K., Bhumiratana, S., Chan, M.E., Cannizzaro, C., Wan, L.Q., Liu, X.S., Guo, X.E., and Vunjak-Novakovic, G. Engineering anatomically shaped human bone grafts. Proc Natl Acad Sci U S A **107,** 2010.
11. Bjerre, L., Bunger, C.E., Kassem, M., and Mygind, T. Flow perfusion culture of human mesenchymal stem cells on silicate-substituted tricalcium phosphate scaffolds. Biomaterials **29,** 2008.
12. Zhao, F., Chella, R., and Ma, T. Effects of shear stress on 3-D human mesenchymal stem cell construct development in a perfusion bioreactor system: experiments and hydrodynamic modeling. Biotechnol Bioeng **96,** 2007.
13. Li, X., Li, D., Wang, L., Lu, B., and Wang, Z. Osteoblast cell response to beta-tricalcium phosphate scaffolds with controlled architecture in flow perfusion culture system. J Mater Sci Mater Med **19,** 2008.
14. Ho, A.D., Wagner, W., and Franke, W. Heterogeneity of mesenchymal stromal cell preparations. Cytotherapy **10,** 2008.

15. Wagner, W., and Ho, A.D. Mesenchymal stem cell preparations—comparing apples and oranges. Stem Cell Rev **3,** 2007.
16. Bonab, M.M., Alimoghaddam, K., Talebian, F., Ghaffari, S.H., Ghavamzadeh, A., and Nikbin, B. Aging of mesenchymal stem cell *in vitro*. BMC Cell Biol **7,** 2006.
17. Baxter, M.A., Wynn, R.F., Jowitt, S.N., Wraith, J.E., Fairbairn, L.J., and Bellantuono, I. Study of telomere length reveals rapid aging of human marrow stromal cells following in vitro expansion. Stem Cells **22,** 2004.
18. Wagner, W., Horn, P., Castoldi, M., Diehlmann, A., Bork, S., Saffrich, R., Benes, V., Blake, J., Pfister, S., Eckstein, V., and Ho, A.D. Replicative senescence of mesenchymal stem cells: a continuous and organized process. PLoS ONE **3,** e2213, 2008.
19. Kim, J., Kang, J.W., Park, J.H., Choi, Y., Choi, K.S., Park, K.D., Baek, D.H., Seong, S.K., Min, H.K., and Kim, H.S. Biological characterization of long-term cultured human mesenchymal stem cells. Arch Pharm Res **32,** 2009.
20. Stolzing, A., Jones, E., McGonagle, D., and Scutt, A. Age-related changes in human bone marrow-derived mesenchymal stem cells: consequences for cell therapies. Mech Ageing Dev **129,** 2008.
21. Sottile, V., Thomson, A., and McWhir, J. In vitro osteogenic differentiation of human ES cells. Cloning Stem Cells **5,** 2003.
22. Bigdeli, N., de Peppo, G.M., Lenneras, M., Sjovall, P., Lindahl, A., Hyllner, J., and Karlsson, C. Superior osteogenic capacity of human embryonic stem cells adapted to matrix-free growth compared to human mesenchymal stem cells. Tissue Eng Part A **16,** 2010.
23. Przyborski, S.A. Differentiation of human embryonic stem cells after transplantation in immune-deficient mice. Stem Cells **23,** 2005.
24. Xu, C., Jiang, J., Sottile, V., McWhir, J., Lebkowski, J., and Carpenter, M.K. Immortalized fibroblast-like cells derived from human embryonic stem cells support undifferentiated cell growth. Stem Cells **22,** 2004.
25. Barberi, T., Willis, L.M., Socci, N.D., and Studer, L. Derivation of multipotent mesenchymal precursors from human embryonic stem cells. PLoS Med **2,** e161, 2005.
26. Lian, Q., Lye, E., Suan Yao, K., Khia Way Tan, E., Salto-Tellez, M., Liu, T.M., Palanisamy, N., El Oakley, R.M., Lee, E.H., Lim, B., and Lim, S.K. Derivation of clinically compliant MSCs from Cd105+, Cd24- differentiated human ESCs. Stem Cells **25,** 2007.
27. Mateizel, I., De Becker, A., Van de Velde, H., De Rycke, M., Van Steirteghem, A., Cornelissen, R., Van der Elst, J., Liebaers, I., Van Riet, I., and Sermon, K. Efficient differentiation of human embryonic stem cells into a homogeneous population of osteoprogenitor-like cells. Reprod Biomed Online **16,** 2008.
28. Olivier, E.N., Rybicki, A.C., and Bouhassira, E.E. Differentiation of human embryonic stem cells into bipotent mesenchymal stem cells. Stem Cells **24,** 2006.
29. Hwang, N.S., Varghese, S., Lee, H.J., Zhang, Z., Ye, Z., Bae, J., Cheng, L., and Elisseeff, J. In vivo commitment and functional tissue regeneration using human embryonic stem cell-derived mesenchymal cells. Proc Natl Acad Sci U S A **105,** 2008.
30. Karlsson, C., Emanuelsson, K., Wessberg, F., Kajic, K., Axell, M.Z., Eriksson, P.S., Lindahl, A., Hyllner, J., and Strehl, R. Human embryonic stem cell-derived mesenchymal progenitors-potential in regenerative medicine. Stem Cell Res **3,** 39, 2009.
31. de Peppo, G.M., Svensson, S., Lenneras, M., Synnergren, J., Stenberg, J., Strehl, R., Hyllner, J., Thomsen, P., and Karlsson, C. Human embryonic mesodermal progenitors highly resemble human mesenchymal stem cells and display high potential for tissue engineering applications. Tissue Eng Part A **16,** 2010.
32. de Peppo, G.M., Sjovall, P., Lenneras, M., Strehl, R., Hyllner, J., Thomsen, P., and Karlsson, C. Osteogenic potential of human mesenchymal stem cells and human embryonic stem cell-derived mesodermal progenitors: a tissue engineering perspective. Tissue Eng Part A **16,** 2010.
33. Guillemin, G., Meunier, A., Dallant, P., Christel, P., Pouliquen, J.C., and Sedel, L. Comparison of coral resorption and bone apposition with two natural corals of different porosities. J Biomed Mater Res **23,** 1989.
34. Irigaray, J.L., Oudadesse, H., Fadl, H., Sauvage, T., Thomas, G., and Vernay, A.M. Effet de la temperature sur la structure cristalline d'un biocorail. J Therm Anal Calorim **39,** 1993.
35. David, B., Bonnefont-Rousselot, D., Oudina, K., Degat, M.C., Deschepper, M., Viateau, V., Bensidhoum, M., Oddou, C., and Petite, H. A perfusion bioreactor for engineering bone constructs: an in vitro and in vivo study. Tissue Eng Part C Methods **17,** 2011.
36. Cruel, M. Effet des contraintes mécaniques sur les cultures cellulaires en ingénierie tissulaire osseuse [Master of Science thesis]. Ecole nationale supérieure des Mines de Saint-Etienne, 2011.
37. Zhao, F., and Ma, T. Perfusion bioreactor system for human mesenchymal stem cell tissue engineering: dynamic cell seeding and construct development. Biotechnol Bioeng **91,** 2005.
38. Kim, H.J., Kim, U., Leisk, G.G., Bayan, C., Georgakoudi, I., and Kaplan, D.L. Bone regeneration on macroporous aqueous-derived silk 3-D scaffolds. Macromol Biosci **7,** 2007.
39. Stiehler, M., Bünger, C., Baatrup, A., Lind, M., Kassem, M., and Mygind, T. Effect of dynamic 3-D culture on proliferation, distribution, and osteogenic differentiation of human mesenchymal stem cells. J Biomed Mater Res A **89,** 2009.
40. Meinel, L., Karageorgiou, V., Fajardo, R., Snyder, B., Shinde-Patil, V., Zichner, L., Kaplan, D., Langer, R., and Vunjak-Novakovic, G. Bone tissue engineering using human mesenchymal stem cells: effects of scaffold material and medium flow. Ann Biomed Eng **32,** 2004.
41. Mygind, T., Stiehler, M., Baatrup, A., Li, H., Zou, X., Flyvbjerg, A., Kassem, M., and Bunger, C. Mesenchymal stem cell ingrowth and differentiation on coralline hydroxyapatite scaffolds. Biomaterials **28,** 2007.
42. Kapur, S., Baylink, D.J., and Lau, K.H. Fluid flow shear stress stimulates human osteoblast proliferation and differentiation through multiple interacting and competing signal transduction pathways. Bone **32,** 2003.
43. Hu, G., Quaranta, V., and Li, D. Modeling of effects of nutrient gradients on cell proliferation in microfluidic bioreactor. Biotechnol Prog **23,** 2007.
44. Holzwarth, C., Vaegler, M., Gieseke, F., Pfister, S.M., Handgretinger, R., Kerst, G., and Muller, I. Low physiologic oxygen tensions reduce proliferation and differentiation of human multipotent mesenchymal stromal cells. BMC Cell Biol **11,** 2010.
45. Holtorf, H.L., Datta, N., Jansen, J.A., and Mikos, A.G. Scaffold mesh size affects the osteoblastic differentiation of seeded marrow stromal cells cultured in a flow perfusion bioreactor. J Biomed Mater Res A **74,** 2005.

46. Lynch, M.P., Capparelli, C., Stein, J.L., Stein, G.S., and Lian, J.B. Apoptosis during bone-like tissue development in vitro. J Cell Biochem **68,** 1998.
47. Yano, S., Komine, M., and Fujimoto, M. Mechanical stretching *in vitro* regulates signal transduction pathways and cellular proliferation in human epidermal keratinocytes. J Invest Dermatol **122,** 2004.
48. Kern, B., Shen, J., Starbuck, M., and Karsenty, G. Cbfa1 contributes to the osteoblast-specific expression of type I collagen genes. J Biol Chem **276,** 2001.
49. Foo, L.H., Suzina, A.H., Azlina, A., and Kannan, T.P. Gene expression analysis of osteoblasts seeded in coral scaffold. J Biomed Mater Res A **87,** 2008.
50. Siffert, R.S. The role of alkaline phosphatase in osteogenesis. J Exp Med **93,** 1951.
51. Fraser, H.B., Hirsh, A.E., Giaever, G., Kumm, J., and Eisen, M.B. Noise minimization in eukaryotic gene expression. PLoS Biol **2,** e137, 2004.
52. Moss, D.W. Release of membrane-bound enzymes from cells and the generation of isoforms. Clin Chim Acta **226,** 1994.
53. Roach, H.I. Why does bone matrix contain non-collagenous proteins? the possible roles of osteocalcin, osteonectin, osteopontin and bone sialoprotein in bone mineralisation and resorption. Cell Biol Int **18,** 1994.
54. Lian, J.B., Stein, G.S., Stein, J.L., Van Wijnen, A., McCabe, L., Banerjee, C., and Hoffmann, H. The osteocalcin gene promoter provides a molecular blueprint for regulatory mechanisms controlling bone tissue formation: role of transcription factors involved in development. Connect Tissue Res **35,** 1996.
55. Lian, J.B., Stein, G.S., Stein, J.L., and van Wijnen, A.J. Osteocalcin gene promoter: unlocking the secrets for regulation of osteoblast growth and differentiation. J Cell Biochem Suppl **30–31,** 1998.
56. Ducy, P., Desbois, C., Boyce, B., Pinero, G., Story, B., Dunstan, C., Smith, E., Bonadio, J., Goldstein, S., Gundberg, C., Bradley, A., and Karsenty, G. Increased bone formation in osteocalcin-deficient mice. Nature **382,** 1996.
57. Wang, L., Hu, Y.Y., Wang, Z., Li, X., Li, D.C., Lu, B.H., and Xu, S.F. Flow Perfusion culture of human fetal bone cells in large beta-tricalcium phosphate scaffold with controlled architecture. J Biomed Mater Res A **91,** 2009.
58. Scaglione, S., Wendt, D., Miggino, S., Papadimitropoulos, A., Fato, M., Quarto, R., and Martin, I. Effects of fluid flow and calcium phosphate coating on human bone marrow stromal cells cultured in a defined 2D model system. J Biomed Mater Res A **86,** 2008.
59. Liu, F., Malaval, L., and Aubin, J.E. The mature osteoblast phenotype is characterized by extensive plasticity. Exp Cell Res **232,** 1997.
60. Eriksson, C., Malmberg, P., and Nygren, H. Time-of-flight secondary ion mass spectrometric analysis of the interface between bone and titanium implants. Rapid Commun Mass Spectrom **22,** 2008.
61. Malmberg, P., and Nygren, H. Methods for the analysis of the composition of bone tissue, with a focus on imaging mass spectrometry (Tof-Sims). Proteomics **8,** 2008.

Address correspondence to:
Giuseppe Maria de Peppo, Ph.D.
The New York Stem Cell Foundation
3960 Broadway, 4th floor
Room 440B
New York, NY 10032

E-mail: gdepeppo@nyscf.org; gm2508@columbia.edu

Received: July 20, 2012
Accepted: July 30, 2012
Online Publication Date: October 1, 2012